



Rivers as linear elements in landform evolution models

Stefan Hergarten¹

¹Institut für Geo- und Umweltnaturwissenschaften, Albertstr. 23B, 79104 Freiburg, Germany

Correspondence: Stefan Hergarten
(stefan.hergarten@geologie.uni-freiburg.de)

Abstract. Models of detachment-limited fluvial erosion have a long history in landform evolution modeling in mountain ranges. However, they suffer from a scaling problem when coupled to models of hillslope processes due to the flux of material from the hillslopes into the rivers. This scaling problem causes a strong dependence of the resulting topographies on the spatial resolution of the grid. A few attempts based on the river width have been made in order to avoid the scaling problem, but none of them appears to be completely satisfying. Here a new scaling approach is introduced that is based on the size of the hillslope areas in relation to the river network. An analysis of several simulated drainage networks yields a power-law scaling relation for the fluvial incision term involving the threshold catchment size where fluvial erosion starts and the mesh width. The obtained scaling relation is consistent with the concept of the steepness index and does not rely on any specific properties of the model for the hillslope processes.

10 1 Introduction

Fluvial incision is a major if not even dominant component of long-term landform evolution in orogens. When modeling fluvial erosion, restriction to the detachment-limited regime considerably simplifies the equations. Here it is assumed that the erosion rate at any point of a river can be predicted from local properties such as discharge and slope, while sediment transport is not considered. The generic differential equation for the topography $H(x_1, x_2, t)$ of a landform evolution model with detachment-limited fluvial erosion reads

$$\frac{\partial H}{\partial t} = U - E - \text{div} \mathbf{q} \quad (1)$$

where U is the uplift rate and E the rate of fluvial incision. The third term describes a local transport process at the hillslopes where \mathbf{q} is the flux density and div the 2D divergence operator. Linear diffusion is the simplest model here; it was considered in the context of landform evolution by Culling (1960) even before models of fluvial erosion came into play. However, there are also more sophisticated models for \mathbf{q} taking into account the nonlinear dependencies of hillslope processes on topography.

Concerning the fluvial incision term E , assuming a power-law function of the catchment size A and the channel slope S ,

$$E = KA^m S^n, \quad (2)$$

has become some kind of paradigm. The parameter K is denoted erodibility. Since this relation should in principle rather involve discharge instead of catchment size, it is only an approximation for constant precipitation, and K is a lumped parameter



25 combining rock properties with precipitation. However, writing Eq. (2) in terms of discharge instead of catchment size is quite straightforward, so that predicting the spatial distribution of precipitation on a changing topography is the only challenge here.

Equation (2) is often called stream power approach since it can be interpreted in terms of energy dissipation of the water per channel bed area if an empirical relationship between channel width and catchment size is used (e.g., Whipple and Tucker, 1999). However, the idea behind this approach even dates back to the empirical study of longitudinal channel profiles by Hack
30 (1957). In this study, a power-law relationship between channel slope and drainage area was found, often called Flint's law (Flint, 1974). This relationship is nowadays usually written in the form

$$S = k_s A^{-\theta} \quad (3)$$

where θ is the concavity index and k_s the steepness index. This relation predicts $\frac{m}{n} = \theta$ and allows for a convenient interpretation of the erodibility. If local transport (last term in Eq. 1) is neglected, the steepness index of a steady-state river (equilibrium
35 of uplift and fluvial incision) follows the relation

$$k_s^n = \frac{U}{K}. \quad (4)$$

This relation allows for a simple adjustment of the lumped parameter K in such a way that a given channel steepness is achieved in equilibrium with a given uplift rate.

2 The scaling problem

40 While widely used and in principle simple, all models of the type described by Eqs. (1) and (2) suffer from a scaling problem. Mathematically, the problem is that catchment sizes are not well-defined in the continuum limit as the catchment of each point degenerates to a line. When considered on a discrete grid, rivers become linear objects with a width of one pixel. Thus, the total area covered by large rivers decreases with decreasing mesh width. As a consequence, the area where uplift can be balanced by fluvial erosion at moderate channel slopes also decreases, so that the overall topography becomes steeper.

45 If local transport is not considered, the scaling problem leads to a canyon-like topography where the width of the valleys decreases with mesh width. However, the rivers still follow Eqs. (3) and (4), so that the scaling problem may not be crucial. But as soon as local transport comes into play, it also affects the rivers. Then the topography becomes strongly dependent on the mesh width.

The problem has been known and addressed for more than 25 years. Howard (1994) suggested a subpixel representation
50 of the rivers where a river segment only covers a fraction of a grid cell. It was assumed that this fraction is $\frac{w}{\delta}$ where w is the river width and δ the mesh width of the grid, and then the fluvial incision term E was multiplied with this factor. While straightforward at first sight, this scaling approach is not free of problems. The channel width in general increases in downstream direction, so that equilibrium river profiles are no longer consistent with Eq. (3) if E is rescaled without further modifications. As discussed by Pelletier (2010), the exponent m must be lowered in order to keep it consistent. In this case, the
55 physical unit of the erodibility K changes, which destroys its relation to the channel steepness. Assuming a constant channel



width w (e.g., Perron et al., 2008) introduces a dimensional parameter without a physical meaning and is practically equivalent to replacing K by wK . So the unit of K also changes in principle, and the problem remains basically the same.

In order to overcome this problem, Pelletier (2010) suggested to leave the fluvial incision term as is and rescale the local transport term (last term in Eq. 1) by the inverse factor $\frac{\delta}{w}$. This formally avoids the problems discussed above, but it might be
60 questionable whether a problem obviously coming from the fluvial incision term can be fixed by rescaling another term in the equation, in particular whether this works for all types of local transport.

So there seems to be no completely satisfying solution of the scaling problem so far. For large mesh widths δ and for rather qualitative studies (e.g., Wulf et al., 2019), it may not be crucial. However, even the comprehensive study on the scaling behavior of fluvial erosion in combination with hillslope diffusion by Theodoratos et al. (2018) disregards the problem by
65 claiming that it dissolves if the entire equation is transformed to nondimensional coordinates. This is, however, not true as the grid spacing δ persists as an additional length scale.

Other recent approaches navigate around the scaling problem by neglecting the flux of material from the hillslopes into the rivers. The recently presented landform evolution model TTLEM (Campforts et al., 2017) makes a distinction by catchment size in such a way that fluvial erosion only acts on sites with a catchment size above a given threshold A_c , while hillslope processes
70 only act at smaller catchment sizes. It is assumed that all hillslope material entering the rivers is immediately excavated without any further effect, so that fluxes from hillslopes into rivers can be disregarded, and the scaling problem does not occur. This approach reduces the interaction between rivers and hillslopes to a one-way coupling where only the rivers have an influence on the evolution of the hillslopes and can be seen as an implementation of bedrock incision in the strict sense. While it seems that the terms detachment-limited erosion and bedrock incision are sometimes used synonymously, it should be clarified that the
75 applicability of the concept of bedrock incision in this strict sense is probably much narrower than that of detachment-limited erosion. The same in principle holds for the model most widely used in the context of drainage divide migration (Goren et al., 2014) where analytical solutions for hillslope processes are used on the sub-pixel scale.

3 A new scaling approach

The scaling issue can be unraveled by reconsidering the empirical basis of Eq. (2). If fluxes of material from the hillslopes
80 into the rivers are not disregarded, the equilibrium of uplift and erosion must be reinterpreted. Erosion at the hillslopes must keep up with fluvial incision in order not to form deeper and deeper canyons. Fluvial incision is the only process in Eq. (1) that immediately removes material, while the last term describing local transport is conservative and thus preserves the total volume. Therefore, the volume per time carried away by a river segment is not the product of the rate defined by Eq. 2 with the area of the river bed, but the product with this area plus a certain hillslope area. An estimate of this area will be developed in
85 this section, and it will finally yield a new scaling relation for the rate of incision as a function of the grid spacing.

In a first step, grid cells belonging to river segments must be distinguished from grid cells interpreted as hillslopes where only local transport takes place. The simplest approach to implement such a distinction is defining a threshold catchment size A_c in such a way that all sites with $A \geq A_c$ are river segments, while all grid cells with $A < A_c$ are hillslope sites. Then the

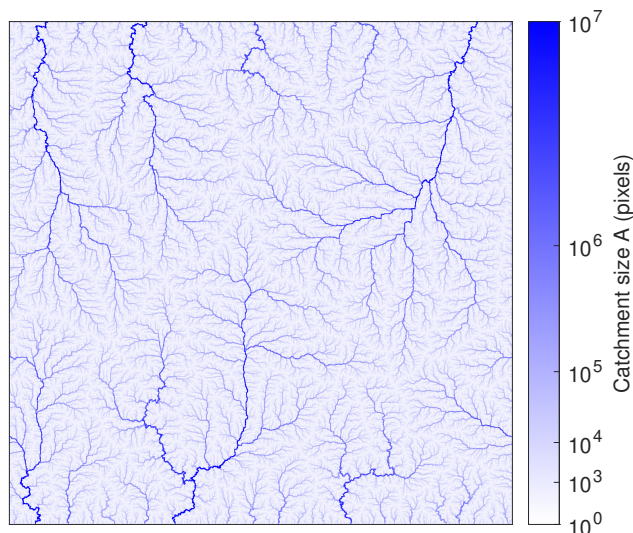


Figure 1. Drainage pattern of a fluvial equilibrium topography computed on a $10,000 \times 10,000$ grid. For clarity, the image was reduced to 2000×2000 pixels taking the highest catchment size within each 5×5 tile.

question is how many hillslopes sites deliver their eroded material to a given river site. This number plus one (for the river site
 90 itself) is the number of sites that have to be eroded by the considered river site. Let us call this number A_e . The expression for
 the fluvial erosion rate (Eq. 2) must then to be modified according to

$$E = A_e K A^m S^n. \quad (5)$$

In the following, numerically obtained equilibrium drainage networks are analyzed in order to find out how A_e depends on
 A and on A_c . These networks were obtained from the landform evolution model OpenLEM that was used in some previous
 95 studies (e.g., Robl et al., 2017; Wulf et al., 2019), but has not been published explicitly. Starting point of the analysis is a
 square $L \times L$ grid with $L = 10000$ where the northern and southern boundaries are held at zero elevation, while the western
 and eastern boundaries are periodic. The simulation was started from a flat topography with a small random disturbance and a
 constant uplift rate. A concavity index of $\theta = 0.5$ as originally suggested by Hack (1957) and an exponent $n = 1$ were assumed.
 The drainage network of the obtained steady-state topography is shown in Fig. 1.

100 Figure 2 reveals that the eroded area A_e increases with the fluvial threshold A_c , but becomes independent of A if the
 catchment size A is sufficiently large. This means that the hillslopes draining to large rivers are not systematically larger than
 those draining to small rivers. It is the reason why we will arrive at a scaling relation that preserves the form of Eq. (2) and
 avoids the problem occurring if the river width is used for scaling.

The increase of A_e if A approaches A_c can be explained by distinguishing between river segments and channel heads. Let us
 105 define channel heads as those sites without any tributary with $A \geq A_c$, i.e., as those sites that are only supplied by hillslopes.
 All other sites with $A \geq A_c$ are considered as river segments. All sites with $A = A_c$ are channel heads and thus follow the
 relation $A_e = A$, so that all curves start at the dotted line in Fig. 2. The resulting values A_e of the river segments (without the

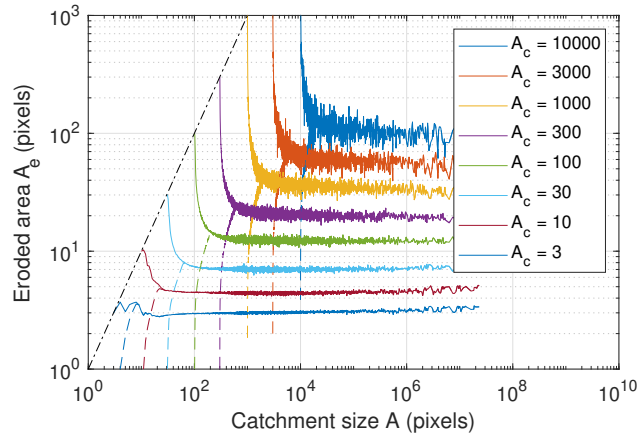


Figure 2. Eroded area A_e as a function of the catchment size A for different fluvial thresholds A_c . Raw data were used for those catchment sizes that occurred at least 1000 times on the grid. Otherwise, data were binned dynamically so that there are at least 1000 points in each bin.

channel heads) are shown by the dashed lines in Fig. 2. The increase of A_e if A approaches A_c even turns into a decrease then. This decrease arises from the limitation $A_e \leq A - A_c$ that holds for all river segments as those have at least one tributary cell contributing at least A_c . So the contribution of the hillslopes must be small if A is only slightly larger than A_c . However, the decrease is exaggerated by the logarithmic scale and concerns only a small number of sites. So it makes sense to assume that A_e is independent of A for river segments.

Both the number of river segment sites and the number of channel head sites decrease with increasing threshold A_c . The decrease of the latter is faster, so that the ratio of the numbers of head sites vs. river sites converges to zero for large A_c . This is, however, not true for the total contributions. Figure 3 shows the ratio of the sum of the A_e values of all river segments and the sum of the A_e values of the channel heads. It can also be interpreted as the ratio of the total area that must be eroded by the river segments over the total area that must be eroded by the channel heads. The results shown for different grid sizes shown in Fig. 3 suggests that this ratio becomes constant in the limit of large grid sizes. It apparently approaches a value of about 2 here, which means that the river segments contribute about two thirds to total fluvial erosion and the channel heads one third.

This result suggests that the dependency of A_e on the threshold A_c is determined by the cumulative distribution $P(A)$ of the catchment sizes in the drainage network. This distribution describes the probability that a randomly selected size has a catchment size $\geq A$. Then a fraction $P(A_c)$ must erode a given fraction (here about two thirds) of the total considered domain, leading to the relation

$$A_e = \frac{\gamma}{P(A_c)} \quad (6)$$

with $\gamma \approx \frac{2}{3}$ for this network. While A_e can be measured directly for the considered drainage network, its relation to $P(A)$ (Eq. 6) is useful as this distribution has already been investigated in several studies on natural and modeled drainage networks (Rodriguez-Iturbe et al., 1992a; Maritan et al., 1996b; Rodriguez-Iturbe and Rinaldo, 1997; Rinaldo et al., 1998; Hergarten and

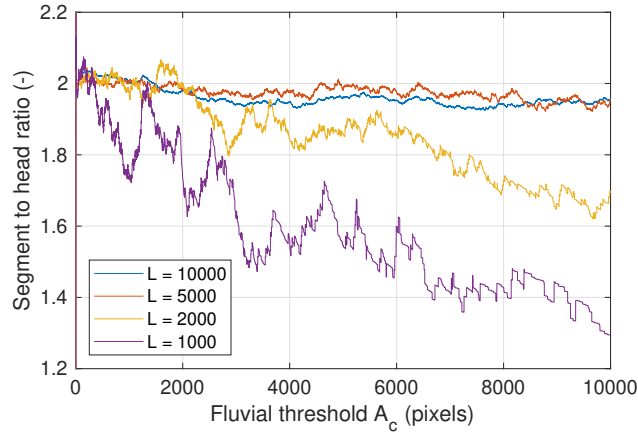


Figure 3. Ratio of total area eroded by all river segments and total area eroded by all channel head sites as a function of the fluvial threshold A_c .

Neugebauer, 2001; Hergarten, 2002; Hergarten et al., 2014, 2016). It was found that $P(A)$ follows a power-law distribution

$$P(A) \sim A^{-\beta} \quad (7)$$

130 over a reasonable range where a range $\beta \in [0.41, 0.46]$ was found except for the two latest studies. In these studies, larger networks were considered making use of increasing data availability and computing capacities. An exponent very close to 0.5 was found for both optimal channel networks (OCNs, see below) (Hergarten et al., 2014) and a real river pattern at the continental scale (Hergarten et al., 2016).

Equations (6) and (7) suggest a power-law relation

$$135 \quad A_e = \alpha A_c^\beta \quad (8)$$

between the eroded area and the fluvial threshold. The validity of Eqs. (6), (7), and (8) is validated in Fig. 4. Comparing the two solid curves reveals that Eq. (6) does not hold exactly since the curves come closer to each other for decreasing catchment sizes. The reason is that A_e only refers to the river segments without the channel heads, so that $P(A_c)$ in Eq. (6) should also exclude the channel head sites. The dashed red line in Fig. 4 showing the accordingly reduced distribution $P(A)$ illustrates that
 140 Eq. (6) indeed holds then, and that the effect vanishes for large A_c .

The black dashed line in Fig. 4 refers to the best-fit power-law relation according to Eq. (8). It is based on all integer values of A_c from 1 to 10,000 assuming equal errors, so that the large values of A_c practically have a high weight in the fit. The power law with the obtained values $\alpha = 1.360$ and $\beta = 0.465$ fits the data well with a relative error of less than 5 % for $A_c \in [15, 10000]$ and less than 1 % for $A_c \in [400, 10000]$. The deviations are larger for smaller fluvial thresholds due to the fact that dendritic
 145 networks cannot be represented well on a regular lattice at small scales.

The relation to the catchment-size distribution (Eqs. 6 and 7) suggests that the power-law dependency of A_e on A_c (Eq. 8) should be universal. For testing this hypothesis, a set of equilibrium topographies with $\theta \in \{0.25, 0.45, 0.5, 0.75\}$ was analyzed.

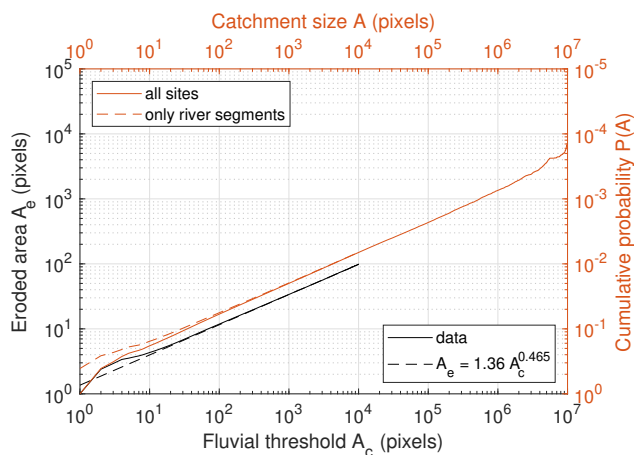


Figure 4. Black axes: eroded area as a function of the fluvial threshold. Red axes: cumulative distribution of the catchment sizes.

These values cover the range that has been found so far under relatively homogeneous conditions (e.g., Robl et al., 2017). The value $\theta = 0.45$ was added as it is often used as a reference value instead of $\theta = 0.5$ (e.g., Whipple et al., 2013; Lague, 2014).

150 Since the exponent n has no immediate effect on equilibrium topographies, values $n \neq 1$ were not considered.

The power-law parameters α and β obtained from equilibrium topographies on different lattice sizes L are given in Table 1. In addition, the original data for the largest grids are shown in Fig. 5. The results are overall similar with a tendency to lower exponents β for increasing θ . A notable deviation is only found for the very high concavity index $\theta = 0.75$. Here the slopes become very steep at small catchment sizes, resulting in a slower migration of drainage divides during the simulation (Robl et al., 2017). As a result, the topography reaches a steady state quite soon, so that there is finally less reorganization in the drainage network with regard to the initial random pattern. In this sense, the lower exponents found for $\theta = 0.75$ can be seen as some fingerprint of poorly organized river patterns, but are probably not relevant for the rivers that were the empirical basis of the stream power law. These findings confirm that the concavity index θ has a minor effect on the topology of the drainage networks, although it strongly affects the shape of longitudinal river profiles and thus the topography.

160 In addition, Table 1 and Fig. 5 also contain results obtained from optimal channel networks (OCNs) on a grid with $L = 4096$. Optimal channel networks are derived from the principle of minimum energy dissipation and have been widely used in the context of river networks (e.g., Howard, 1990; Rodriguez-Iturbe et al., 1992c, b; Rinaldo et al., 1992; Maritan et al., 1996a, b; Rinaldo et al., 1998). The networks considered here are those shown in Fig. 1 of Hergarten et al. (2014) where θ is related to the parameter n used there by $\theta = \frac{n-1}{n+1}$. The values of A_e of OCNs are overall slightly higher than those of the equilibrium topographies, and the variation with θ is lower. As OCNs are organized more strongly than drainage networks of arbitrary equilibrium topographies, the lower variability among OCNs is not surprising.

165 These results suggest to define the values $\alpha = 1.508$ and $\beta = 0.478$ obtained from the OCN with $\theta = 0.5$ as reference values. The question is, however, whether such a precision is useful for applications. In particular, $\beta = 0.5$ would be more convenient than lower values. In the considerations made above, A_e and A_c are measured in DEM pixels and are thus nondimensional



Table 1. Parameter values of the power-law relation between eroded area and fluvial threshold (Eq. 8) obtained from different simulated drainage networks.

	θ	L	α	β
	0.25	5000	1.264	0.492
		2000	1.072	0.511
		1000	1.587	0.470
steady-state topographies	0.45	5000	1.273	0.478
		2000	1.586	0.451
		1000	1.047	0.499
steady-state topographies	0.50	10,000	1.360	0.465
		5000	1.434	0.459
		2000	1.807	0.423
		1000	1.579	0.440
steady-state topographies	0.75	10,000	1.653	0.393
		5000	1.715	0.388
		2000	1.433	0.412
		1000	2.179	0.359
OCNs	0.14	4096	1.487	0.480
	0.33		1.626	0.473
	0.50		1.508	0.478
	0.60		1.521	0.475

170 properties. Defining the grid scale δ as the square root of the area of a DEM pixel (which would be the mesh width for a regular square lattice) and considering A_c as a physical (dimensional) area, A_c has to be replaced by $\frac{A_c}{\delta^2}$ in Eq. 8. Then the fluvial erosion rate (Eq.5) turns into

$$E = \alpha \left(\frac{A_c}{\delta^2} \right)^\beta K A^m S^n, \quad (9)$$

so that the fluvial incision term scales like $\delta^{-2\beta}$. For $\beta = 0.5$, the fluvial term scales like $\frac{1}{\delta}$. This is not only convenient, but also leads to basically the same scaling relation assumed by Perron et al. (2008). The only difference is that the term $\alpha\sqrt{A_c}$ occurring here was interpreted as a channel width w and then assumed to be constant for all rivers, so that it lost its physical meaning. So the new formulation of the fluvial incision term also fixes the concern raised by Pelletier (2010) that led to the alternative formulation where the hillslope transport term was rescaled.

In order to estimate α for $\beta = 0.5$, it is helpful to know in which region of Fig. 5 we are in typical model applications. A breakdown of Flint's law (Eq. 3) was reported at catchment sizes between between about 0.1 km² and 5 km² (Montgomery and Foufoula-Georgiou, 1993; Stock and Dietrich, 2003; Wobus et al., 2006). However, channel steepness declines at small

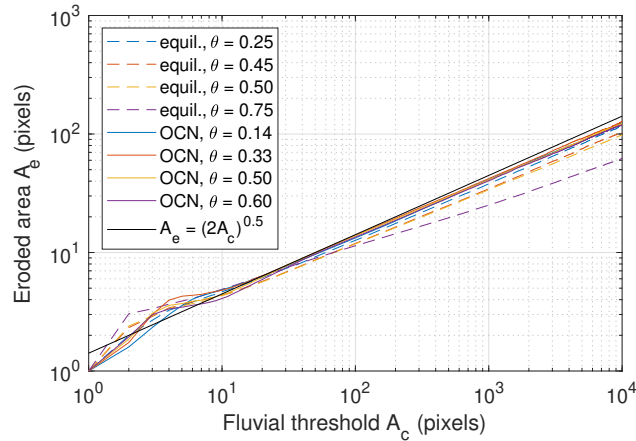


Figure 5. Eroded area A_e as a function of the fluvial threshold A_c for the considered drainage networks. For clarity, only the results obtained from the largest domains are plotted.

catchment sizes, so that this breakdown rather implies that other erosion processes come into play than that fluvial erosion is no longer active. In turn, many springs in mountain regions have subsurface catchment sizes in the order of magnitude of 0.01 km^2 , but it is not clear whether the erosive action of the resulting small streams follows Flint's law. Reasonable estimates
 185 of A_c are probably between these two ranges. Assuming a spatial resolution of about 100 m or a bit less, A_c will be in the order of magnitude of 10 to 100 DEM pixels. As illustrated by the black line in Fig. 5, $\alpha = \sqrt{2}$ provides a reasonable estimate for this range with simple numbers as $\alpha A_c^\beta = \sqrt{2A_c}$ then. With this estimate, the scaling factor for the fluvial erosion rate is $\frac{\sqrt{2A_c}}{\delta}$, and the modified stream-power law for fluvial erosion turns into

$$E = \frac{\sqrt{2A_c}}{\delta} K A^m S^n. \quad (10)$$

190 4 Discussion

The simple scaling relation for the fluvial erosion rate obtained from simulated drainage networks (Eq. 9 or 10) involves some variations in the parameters due to the topology of the drainage network, but appears to be quite universal. Concerning the hillslope processes, Eq. (1) only requires that they are conservative. As fluvial equilibrium topographies were used in the simulations, it was, however, implicitly assumed that the flux of material on the hillslopes follows the same direction as the
 195 flow of water if the hillslopes were part of the fluvial regime. This may not be true since hillslopes are in general smoother than fluvial topographies. However, the scaling relation only depends on the total flux from the hillslopes into the rivers and not on its spatial pattern. Only the relative contributions of river segments and channel head sites may slightly vary, but this should have no big effect. So the scaling relation can indeed be expected to be independent of the specific characteristics of the involved hillslope processes.



200 As the scaling relation originates from the topology of the drainage network, it should also not be limited to the specific form of the stream power law (Eq. 2) used in the simulations. So it should provide a quite general scaling relation for detachment-limited fluvial erosion.

Nevertheless it is important to keep the difference between detachment-limited erosion and bedrock incision in mind. Here it is assumed that the ability of the river to take up particles and carry them away concerns both the river bed and material coming from adjacent hillslopes. If we, conversely, assume that all material coming from the hillslopes is instantaneously removed by the river without any consequences, there is no feedback of the hillslopes to the rivers, and Eq. (1) does not require any rescaling.

5 Conclusions

This study presents a scaling relation for the fluvial incision term in landform evolution models involving detachment-limited fluvial erosion and hillslope processes. In order to avoid a dependence of the simulated topographies on the spatial resolution of the grid, the fluvial incision term must be multiplied by a scaling factor depending on the ratio of the threshold catchment size A_c where fluvial erosion starts and the pixel size δ^2 of the grid. The analysis of several simulated drainage networks yields a power-law dependence of the scaling factor in Eq. (9) with an exponent slightly lower than 0.5. However, for application in numerical models, a simpler approximation where the fluvial erosion rate is rescaled by a factor $\frac{\sqrt{2A_c}}{\delta}$ is suggested.

215 *Code availability.* All codes are available from the author on request.

Author contributions. N/A

Competing interests. The author declares that he has no competing interests.



References

- Campforts, B., Schwanghart, W., and Govers, G.: Accurate simulation of transient landscape evolution by eliminating numerical diffusion: the TTLEM 1.0 model, *Earth Surf. Dynam.*, 5, 47–66, <https://doi.org/10.5194/esurf-5-47-2017>, 2017.
- Culling, W.: Analytical theory of erosion, *J. Geol.*, 68, 336–344, <https://doi.org/10.1086/626663>, 1960.
- Flint, J. J.: Stream gradient as a function of order, magnitude, and discharge, *Water Resour. Res.*, 10, 969–973, <https://doi.org/10.1029/WR010i005p00969>, 1974.
- Goren, L., Willett, S. D., Herman, F., and Braun, J.: Coupled numerical–analytical approach to landscape evolution modeling, *Earth Surf. Process. Landforms*, 39, 522–545, <https://doi.org/10.1002/esp.3514>, 2014.
- Hack, J. T.: Studies of longitudinal profiles in Virginia and Maryland, no. 294-B in US Geol. Survey Prof. Papers, US Government Printing Office, Washington D.C., <https://doi.org/10.3133/pp294B>, 1957.
- Hergarten, S.: Self-Organized Criticality in Earth Systems, Springer, Berlin, Heidelberg, New York, <https://doi.org/10.1007/978-3-662-04390-5>, 2002.
- Hergarten, S. and Neugebauer, H. J.: Self-organized critical drainage networks, *Phys. Rev. Lett.*, 86, 2689–2692, <https://doi.org/10.1103/PhysRevLett.86.2689>, 2001.
- Hergarten, S., Winkler, G., and Birk, S.: Transferring the concept of minimum energy dissipation from river networks to subsurface flow patterns, *Hydrol. Earth Syst. Sci.*, 18, 4277–4288, <https://doi.org/10.5194/hess-18-4277-2014>, 2014.
- Hergarten, S., Winkler, G., and Birk, S.: Scale invariance of subsurface flow patterns and its limitation, *Water Resour. Res.*, 52, 3881–3887, <https://doi.org/10.1002/2015WR017530>, 2016.
- Howard, A. D.: Theoretical model of optimal drainage networks, *Water Resour. Res.*, 26, 2107–2117, <https://doi.org/10.1029/WR026i009p02107>, 1990.
- Howard, A. D.: A detachment-limited model for drainage basin evolution, *Water Resour. Res.*, 30, 2261–2285, <https://doi.org/10.1029/94WR00757>, 1994.
- Lague, D.: The stream power river incision model: evidence, theory and beyond, *Earth Surf. Process. Landforms*, 39, 38–61, <https://doi.org/10.1002/esp.3462>, 2014.
- Maritan, A., Colaiori, F., Flammini, A., Cieplak, M., and Banavar, J. R.: Universality classes of optimal channel networks, *Science*, 272, 984–986, <https://doi.org/10.1126/science.272.5264.984>, 1996a.
- Maritan, A., Rinaldo, A., Rigon, R., Giacometti, A., and Rodriguez-Iturbe, I.: Scaling laws for river networks, *Phys. Rev. E*, 53, 1510–1515, <https://doi.org/10.1103/PhysRevE.53.1510>, 1996b.
- Montgomery, D. R. and Foufoula-Georgiou, E.: Channel network source representation using digital elevation models, *Water Resour. Res.*, 29, 3925–3934, <https://doi.org/10.1029/93WR02463>, 1993.
- Pelletier, J. D.: Minimizing the grid-resolution dependence of flow-routing algorithms for geomorphic applications, *Geomorphology*, 122, 91–98, <https://doi.org/10.1016/j.geomorph.2010.06.001>, 2010.
- Perron, J. T., Dietrich, W. E., and Kirchner, J. W.: Controls on the spacing of first-order valleys, *J. Geophys. Res. Earth Surf.*, 113, F04016, <https://doi.org/10.1029/2007JF000977>, 2008.
- Rinaldo, A., Rodriguez-Iturbe, I., Bras, R. L., Ijjasz-Vasquez, E., and Marani, A.: Minimum energy and fractal structures of drainage networks, *Water Resour. Res.*, 28, 2181–2195, <https://doi.org/10.1029/92WR00801>, 1992.



- Rinaldo, A., Rodriguez-Iturbe, I., and Rigon, R.: Channel networks, *Annu. Rev. Earth Planet. Sci.*, 26, 289–327, 255
<https://doi.org/10.1146/annurev.earth.26.1.289>, 1998.
- Robl, J., Hergarten, S., and Prasicek, G.: The topographic state of fluviually conditioned mountain ranges, *Earth Sci. Rev.*, 168, 290–317,
<https://doi.org/10.1016/j.earscirev.2017.03.007>, 2017.
- Rodriguez-Iturbe, I. and Rinaldo, A.: *Fractal River Basins. Chance and Self-Organization*, Cambridge University Press, Cambridge, New York, Melbourne, 1997.
- 260 Rodriguez-Iturbe, I., Ijjasz-Vasquez, E., Bras, R. L., and Tarboton, D. G.: Power law distribution of mass and energy in river basins, *Water Resour. Res.*, 28, 1089–1093, 1992a.
- Rodriguez-Iturbe, I., Rinaldo, A., Rigon, R., Bras, R. L., Ijjasz-Vasquez, E., and Marani, A.: Fractal structures as least energy patterns: The case of river networks, *Geophys. Res. Lett.*, 19, 889–892, <https://doi.org/10.1029/92GL00938>, 1992b.
- Rodriguez-Iturbe, I., Rinaldo, A., Rigon, R., Bras, R. L., Marani, A., and Ijjasz-Vasquez, E.: Energy dissipation, runoff production, and the 265
three-dimensional structure of river basins, *Water Resour. Res.*, 28, 1095–1103, <https://doi.org/10.1029/91WR03034>, 1992c.
- Stock, J. and Dietrich, W. E.: Valley incision by debris flows: Evidence of a topographic signature, *Water Resour. Res.*, 39, 1089,
<https://doi.org/10.1029/2001WR001057>, 2003.
- Theodoratos, N., Seybold, H., and Kirchner, J. W.: Scaling and similarity of a stream-power incision and linear diffusion landscape evolution model, *Earth Surf. Dynam.*, 6, 779–808, <https://doi.org/10.5194/esurf-6-779-2018>, 2018.
- 270 Whipple, K. X. and Tucker, G. E.: Dynamics of the stream power river incision model: Implications for height limits of mountain ranges, landscape response time scales and research needs, *J. Geophys. Res.*, 104, 17 661–17 674, <https://doi.org/10.1029/1999JB900120>, 1999.
- Whipple, K. X., DiBiase, R. A., and Crosby, B. T.: Bedrock rivers, in: *Fluvial Geomorphology*, edited by Shroder, J. and Wohl, E., vol. 9 of *Treatise on Geomorphology*, pp. 550–573, Academic Press, San Diego, CA, <https://doi.org/10.1016/B978-0-12-374739-6.00226-8>, 2013.
- Wobus, C., Whipple, K. X., Kirby, E., Snyder, N., Johnson, J., Spyropoulou, K., Crosby, B., and Sheehan, D.: Tectonics from topogra- 275
phy: Procedures, promise, and pitfalls, in: *Tectonics, Climate, and Landscape Evolution*, edited by Willett, S. D., Hovius, N., Brandon, M. T., and Fisher, D. M., vol. 398 of *GSA Special Papers*, pp. 55–74, Geological Society of America, Boulder, Washington, D.C., [https://doi.org/10.1130/2006.2398\(04\)](https://doi.org/10.1130/2006.2398(04)), 2006.
- Wulf, G., Hergarten, S., and Kenkmann, T.: Combined remote sensing analyses and landform evolution modeling reveal the terrestrial Bosumtwi impact structure as a Mars-like rampart crater, *Earth. Planet. Sci. Lett.*, 506, 209–220, <https://doi.org/10.1016/j.epsl.2018.11.009>, 280
2019.